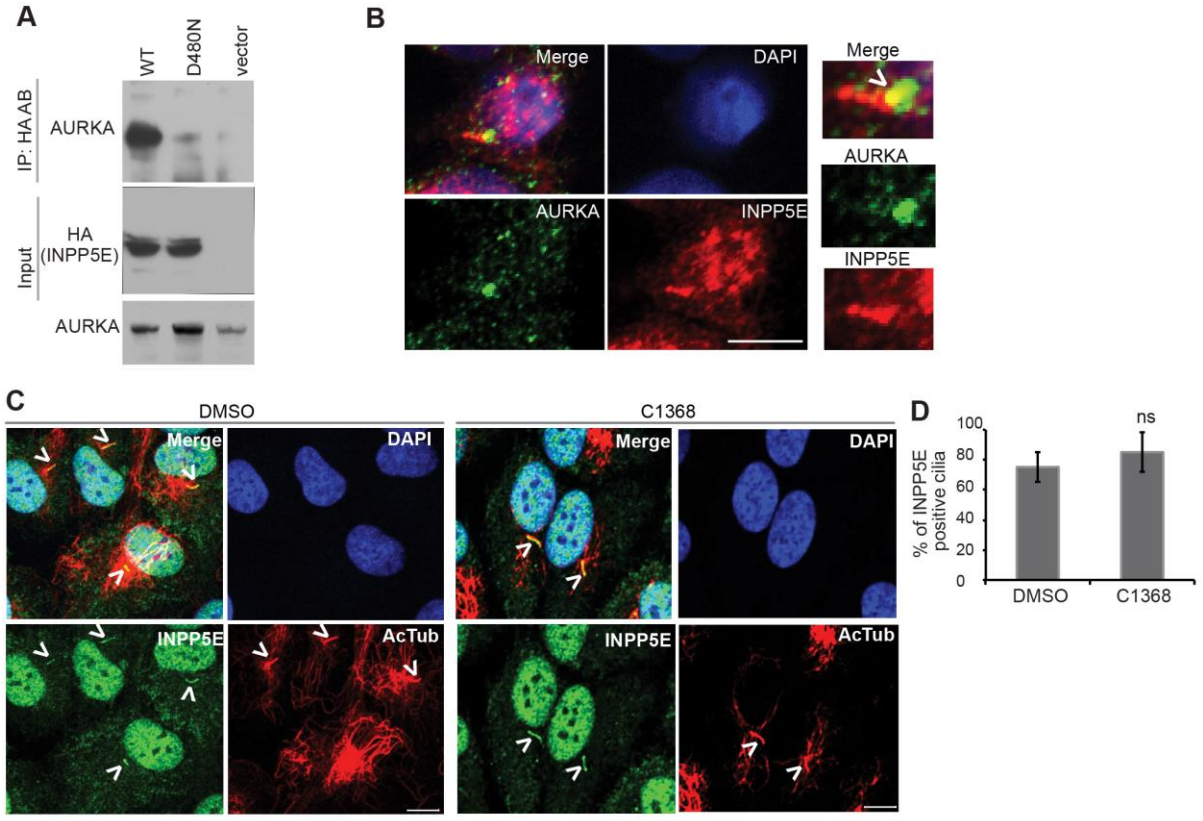

Supplemental Figure 1

(A) Lysates from HEK293 cells expressing HA-INPP5E or catalytically in-active HA-INPP5E D480N mutant and RFP-AURKA were immuno-precipitated and western blotted with the indicated antibodies. (B) Immuno-fluorescence analysis detects AURKA (green) and INPP5E (red) in IMCD3 cells demonstrating basal body localization of AURKA and ciliary axoneme localization of INPP5E, with overlap at basal end of cilium (the colocalization is indicated by arrowhead). DAPI indicates the nucleus (blue). Scale bar, 10 μm. Inserts show magnification of basal body and cilia. (C) Immuno-staining for INPP5E (green) and acetylated α-tubulin (AcTub, red) in ciliated, serum starved, IMCD3 cells 24 h after treatment with 2 μM C1368 for 6 h versus control DMSO cells. (D) Quantification of INPP5E positive cilia after indicated treatments; ns, not significant.

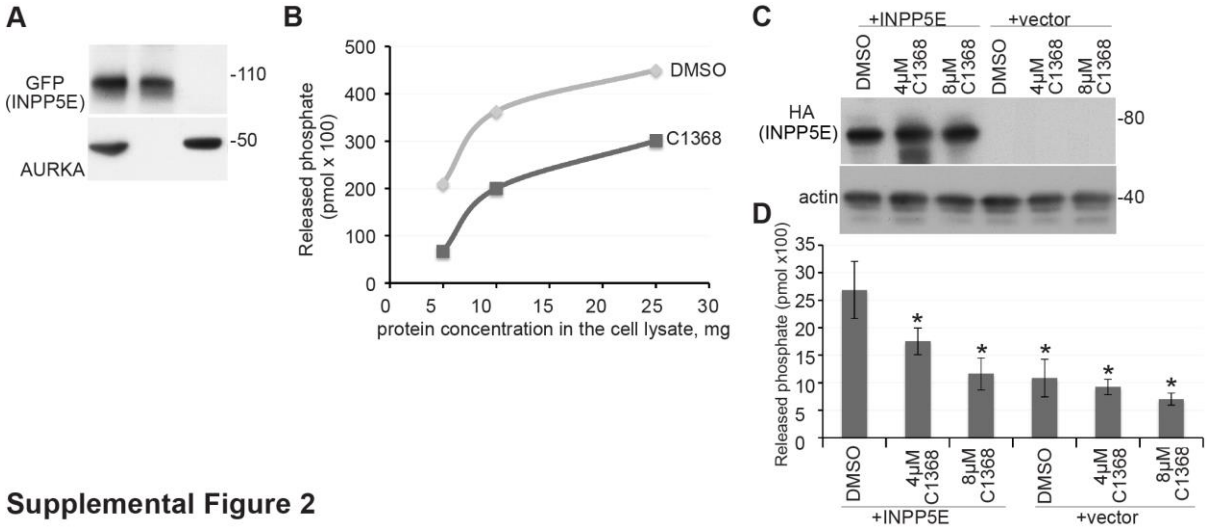

Supplemental Figure 2

(A) Blotting shows presence of indicated recombinant proteins in the reaction mix for the 5-phosphatase assay. (B) Titration of different concentrations of protein lysates obtained from HEK293 cells overexpressing INPP5E and treated for 3 h before lysis with 2 μM C1368 or DMSO control in phosphatase assay. (C) Western blotting shows overexpression of INPP5E in HEK293 cells employed in the phosphatase assay. (D) Quantification of INPP5E 5-phosphatase activity against PtdIns(3,4,5)P3 upon AURKA inhibition with indicated concentrations of C1368 in HEK293 cells overexpressing HA-INPP5E or empty vector, *$p<0.01$.

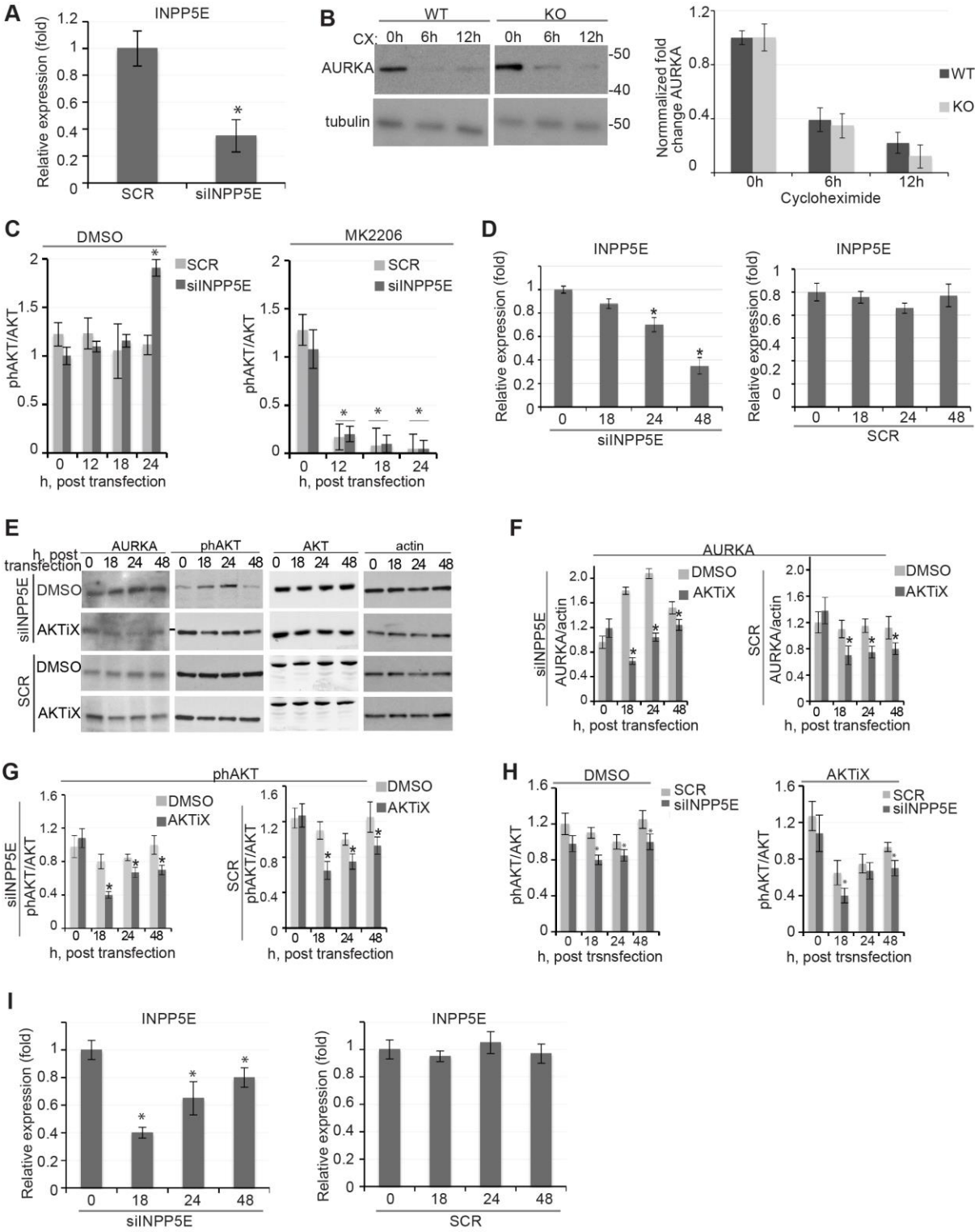

Supplemental Figure 3

(A) mRNA expression levels of *INPP5E* in IMCD3 cells was determined by real-time RT-PCR, and data presented as fold change relative to WT control. Error bars, SEM. *, p=0.013. (B) Western blot analysis of AURKA expression in *Inpp5e*$^{+/+}$ (WT) and *Inpp5e*$^{-/-}$ (-/-) mouse embryonic fibroblasts treated with cycloheximide. Expression was normalized against α-

tubulin. The bottom panel shows quantification of AURKA, n=3, fold of change of AURKA expression to time point 0h, error bars = SEM, $p>0.05$ at each time point; Molecular masses are indicated in kDa. (C) The graph indicates the ratio of phAKT to AKT, quantified from analysis of three blots; error bars = SEM. *, $p<0.01$. Molecular masses are indicated in kDa. (D) mRNA expression levels of *INPP5E* were determined from IMCD3 cells by real-time RT-PCR for Fig 3H,I, and data presented as fold change relative to WT control. Error bars = SEM. *, $p<0.01$. (E) IMCD3 cells were siRNA transfected then treated with AKT inhibitor AKTiX (Bertotti et al., 2009) for 12 hr for all time points as indicated. Lysates were collected and western blotted as indicated. (F,G) The relative phosphorylation of AURKA (F) and AKT (G) were quantified and graphed. Data are expressed as mean values ± SEM of three experiments. (H) The ratio of phAKT to AKT, quantified from analysis of three blots; error bars = SEM. *, $p<0.01$. (I) mRNA expression levels of *INPP5E* were determined from IMCD3 cells by real-time RT-PCR for € and data presented as fold change relative to wild type controls. Error bars, SEM. *, $p<0.01$.

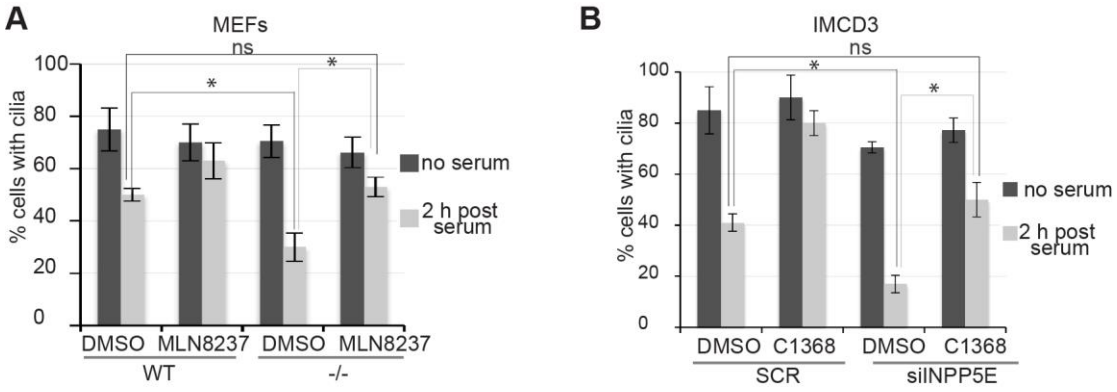

Supplemental Figure 4

(A,B) Embryonic fibroblasts (A) or siRNA-treated IMCD3 cells (B) were grown for 72 or 48 hr in low serum conditions and induced to disassemble cilia in the presence of AURKA inhibitor (0.5 μM MLN8237 for MEFs and 2 μM C1368 for IMCD-3 cells) or DMSO control. The percentage of ciliated cells before and after the indicated treatments is shown. *, $p<0.05$. Three triplicate assays counting 100 cells per assay were performed; error bars = SEM.